Effect of metal oxide precursor on sintering shrinkage, microstructure evolution and electrical properties of silver-based pastes

SAN-YUAN CHEN, CHING-HUAN CHOU
Department of Materials Science and Engineering, National Chiao-Tung University, Hsinchu, Taiwan, Republic of China
E-mail: sychen@cc.nctu.edu.tw

SYH-YUH CHENG
Materials Research Laboratories, Industrial Technology Research Institution, Chutung, Taiwan, Republic of China

Since the shrinkage behavior of silver-based films has been correlated with the characteristics of oxide additives used, the relative role of metal oxides and metal-organic precursors in sintering shrinkage and microstructure evolution of silver films was investigated and compared in this work. Films with an oxide powder additive exhibit two-stage shrinkage behavior in contrast to one-stage continuous shrinkage, which occurs in silver films with metal-organic precursors, added. Furthermore, metal-organic precursors are less effective than metal oxide powders in reducing shrinkage of silver-based films. That can be reasonably explained that metal-organic precursors can be effectively decorated around silver powder to inhibit the sintering densification. The Zr-based organic precursor among the metal-organic precursors exhibits optimal retardation in sintering densification of silver film, which is probably interrelated to refractory characteristics of ZrO_2. The unique conductivity and grain growth of silver film with 1.0 wt% tungsten-organic precursor added was possibly due to the partial dissolution of W into Ag. © *2002 Kluwer Academic Publishers*

1. Introduction

Ceramic dielectric resonators are used as bandpass or bandstop filters and oscillator stabilizer devices in the microwave frequency range of 1 to 12 GHz. These devices are becoming increasingly important with the continued development of microwave integrated circuitry [1–3]. In order to reduce the size of microwave devices in communication systems, the dielectric components must also be miniaturized. Recently, multilayer devices have been developed to increase volume efficiency [4–6]. In multilayer structure, the sintering temperature of microwave dielectric ceramics was necessary to be lowered in order to cofire with low loss conductors such as silver and gold.

A principal problem in multilayer microwave ceramic manufacture originates from the firing of the electrode and dielectric films simultaneously. During firing of multilayer ceramics made with low-firing dielectrics, the electrode film begins to densify. This is due to the presence of large amounts of silver in the film. Silver has a melting point of about 961°C in an inert atmosphere. Dielectrics, which reach complete densification at around 1100°C typically, begin to sinter and shrink at about 800°C to 1000°C. The mismatch between the sintering shrinkage of the electrode and dielectric induces stresses [7–9]. It is known that the addition of metal oxides or glass to the conductor composition can move the sintering shrinkage of the conductive metal powders to higher temperatures and thereby relieve the stresses formed due to differential electrode/dielectric shrinkage [10–12]. However, discontinuous grain growth and Ostwald ripening often take place due to inhomogeneous paricle size distribution. A more effective means of alleviating the mismatch of the sintering shrinkage of the electrode with the dielectric is needed.

A new thick film conductor composition suitable for use for electrodes in multilayer capacitors has been developed [13, 14]. The electrode pastes comprise finely divided particles of electrically conductive metal and an organometallic compound, which is insoluble in the electrically conductive metal in a solution of polymeric binder and volatizable solvent. In some cases, metal-organic compounds of Ru, Rh, Ir or Pt were used to produce better shrinkage matches [15, 16]. However, an onging challenge for future developments in high-performance multilayer microwave ceramics is to reduce the internal electrode cost. Therefore, the development of low-cost metal-based precursors such as Zn, Cu, W, Ni, Zr becomes more important. However, little report was focused on the study of these low-cost metal-organic precursors on sintering shrinkage and microstructure evolution of silver-based films.

 © *2002 Kluwer Academic Publishers*

Therefore, in this paper, first, a variety of metal-organic precursors were selected to compare its role in shrinkage mismatch and microstructure evolution of silver-based pastes. For comparison, metal oxides were also used in the present work. The effect of metal-organic precursors on the conductivity of sintered silver-based films is also investigated in this paper. A possible mechanism will be proposed to explain the shrinkage difference of the silver films with metal-organic precursors and metal oxides added.

2. Experimental procedure

High-purity (more than 99.5%) TiO_2 and $BaCO_3$ were used to prepare $Ba_2Ti_9O_{20}$ ceramics by a conventional powder-processing technique. After the mixture powder was calcined at 1150°C, oxide-based glass was added. The resultant powder was then used to fabricate the dielectric tape by doctor-blade processing.

Spherical silver powder with an average particle size of 1.2 μm was used as the conductive powder in the electrode paste. The metal-organic precursors (abbreviated as MO) used are tungsten isopropoxide (Alfa, designated as MO-W), zinc 2-ethylhexanoate (Alfa, designated as MO-Zn), iron 2-ethylhexanoate (Alfa, designated as MO-Fe), and zirconium 2-ethylhexanoate (Alfa, designated as MO-Zr). The metal oxide content of the metal-organic precursors used in the electrode paste constituted 0.5–2.0 wt% of total silver powder. Ethyl cellulose dissolved in a mixture of 6 wt% beta-terpineol and 74 wt% butyl carbitol acetate was used as an organic medium. In this experiment, the solid content of 75 wt% was used except otherwise noted. Metal oxides including Fe_2O_3, ZnO, ZrO_2 and WO_3 were also used for comparison.

The additives were first stirred into the pastes and then the mixture was roll-milled to ensure maximum dispersion of the additive. Most thick film compositions were applied to the dielectric green tape by means of screen-printing. Subsequently, the screen-printed silver-based pastes were sintered in air at various temperatures for 0.5 h. A two-layer structure with silver-based film in between dielectrics was also used to investigate the cross-section microstructure. The thermal mechanical analysis (TMA) was further used to study the effect of the additives on the sintering shrinkage of the silver-based films. The silver paste was first cast on an alumina substrate and dried at 150°C until all paste solvent was removed. Subsequently, the coated-paste substrate was covered with another alumina plate to construct a sandwich structure for the measurement of shrinkage as a function of temperature. Samples of the fired parts were cross-sectioned after mounting the parts in an epoxy potting compound and then polished to expose the inner structure. The microstructure of the sintered samples was observed using scanning electron microscopy (SEM, Hitachi S4000). The conductive properties of silver-based films at high frequencies were evaluated using conductors patterned on 0.025" thick, 99% alumina substrates with the T-patterns on one surface of the substrate and the return plane on the opposite surface [17]. The transmission response of the T-pattern resonator was measured using a Hewlett Packard 8722D Microwave Network Analyzer System. Measurements of the conductor width, thickness, length, and surface roughness were used to calculate the conductivity of conductors.

3. Results

3.1. Shrinkage of silver film and dielectric tape

Glass-added $Ba_2Ti_9O_{20}$ based compositions were used to fabricate dielectric tape for multilayer microwave. A porous structure composed of fine particle distribution was observed (see Fig. 1), which indicates that little densification occurred for the sample sintered at 800°C. On the other hand, for pure silver powder, the microstructure change of silver film on the dielectric tape was strongly influenced by the firing temperatures as shown in Fig. 2. The shapes of most of the particles become irregular at 400°C (Fig. 2a), and the irregular-shaped particles grow rapidly into large ones at 600°C (Fig. 2b) due to the coalescence of silver particles [18]. With increasing soaking time, the silver films become dense and more grain growth takes place. The black regions in the photographs are voids and become fewer. After the silver film was sintered at 800°C for 0.5 h, a fully dense microstructure, shown in Fig. 2c, exhibiting a regular array of steps was observed. Ali *et al.* [19] reported that as the silver films were deposited on Si(100) substrate and then annealed at 300°C, a (100) oriented silver film was observed. With respect to silver symmetry, it was found that (100) was usually a lower energy plane in FCC structure. Therefore, the formation of layered step structure results mainly from the lower energy plane and the fast migration of silver atoms.

The shrinkage curve of the silver-based films, measured by the TMA with a heating rate of 5°C/min., was used to calculate the percent shrinkage relative to the unfired dried film thickness. Fig. 3 shows the pure silver paste starts to shrink around 400°C. Subsequently, the shrinkage becomes sluggish with sintering temperature over 600°C and ends around 800°C. The shrinkage amount was about 18% and 23% at 600°C and 800°C, respectively. On the other hand, the starting temperature of shrinkage for dielectric ceramic tape was about

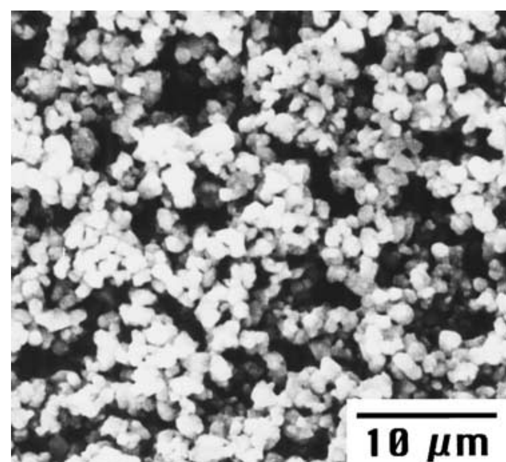

Figure 1 SEM micrograph of dielectric ceramic sintered at 800°C for 0.5 h.

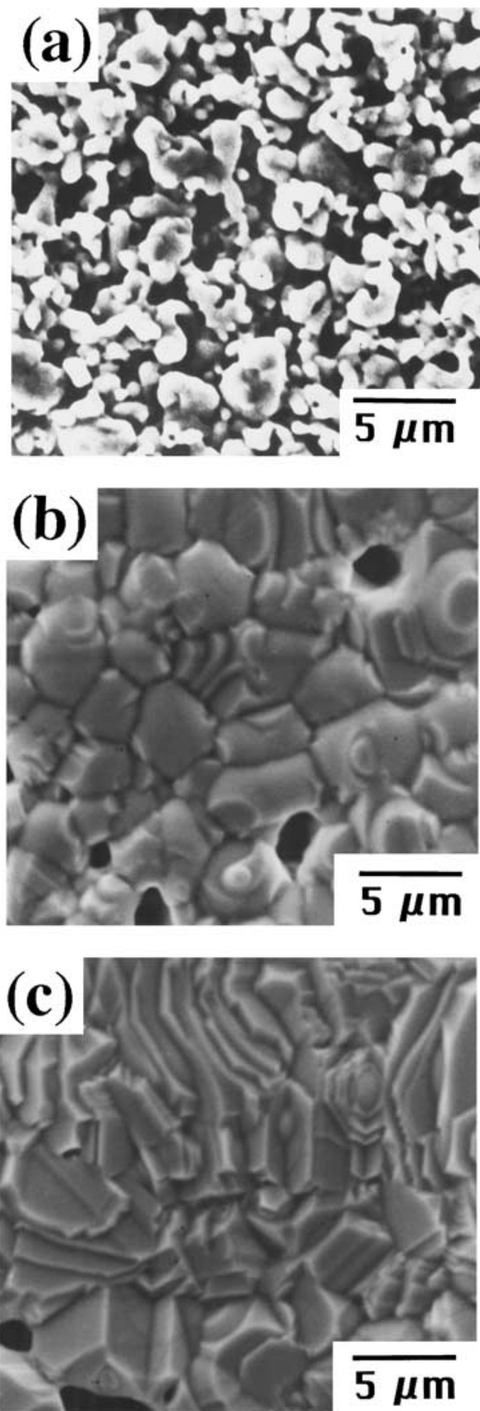

Figure 2 SEM surface microstructure of silver films sintered at (a) 400°C, (b) 600°C and (c) 800°C for 0.5 h.

750–800°C, much higher than that of silver paste. At 800°C, the tape shrank about 3.9%, which were approximately 22% of the final total shrinkage.

3.2. Additive of metal oxide

A variety of metal oxide powders were used to study its effect on the sintering behavior of silver-based films. As shown in Fig. 3, some interesting features can be noticed. First, the TMA curves present two-stage shrinkage. Second, the addition of metal oxides does show effective retardation on the sintering densification of silver film. Third, the ZrO_2 additive presents the optimal retardation on the sintering shrinkage.

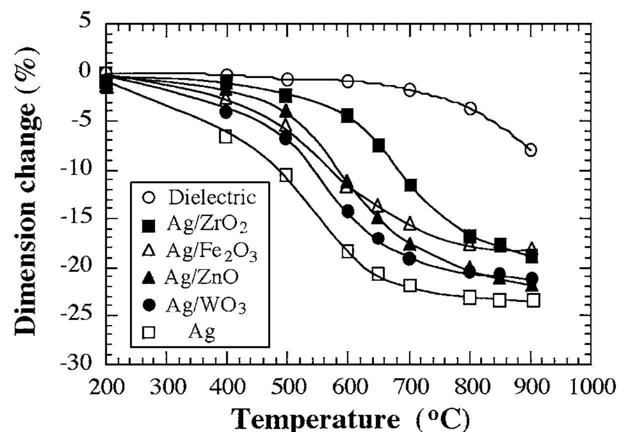

Figure 3 Thermal shrinkage characteristics of silver films with metal oxide added at a heating rate of 5°C/min.

Depending on the addition of metal oxides, the microstructure development of silver-based films was widely varied as shown in Fig. 4. For comparison, both 600°C and 800°C firing temperatures were employed in this work. The microstructure observation shows that WO_3-added silver film presents similar structural change to pure silver film. At 600°C, particle-necking and partial densification occur. As the sintering temperature rises to 800°C, the flat terraces with array of parallel steps were observed (Fig. 4b). Similar microstructure evolution was also observed for Fe_2O_3-added silver film. On the other hand, the SEM micrographs in Fig. 4c show the ZnO particles were widely distributed throughout the silver grains as the film was fired at 600°C. At a higher temperature of 800°C, it was found that ZnO-added silver film presents a completely different microstructure from that of pure silver film. The flat grains with parallel steps were not observed. As the ZrO_2 powder was added to silver films, it was found that at 600°C, Fig. 4d, necking formation took place in between Ag particles. With raising the temperature up to 800°C, it exhibited a porous microstructure and inhomogeneous sintering densification occurred in some aggregated small grains.

3.3. Additive of metal-organic precursor

For comparison, the metal-organic precursors were added to silver powder to study its effect on the sintering shrinkage of silver films. As shown in Fig. 5, the shrinkage curves present a smooth and continuous change with increasing sintering temperature instead of two-stage curves as observed in the Fig. 3 for oxide additives. The shrinkage behavior of silver film with MO-W added was very similar to that of pure silver film. Furthermore, the addition of MO-W apparently promotes sintering instead of retardation in that it produced more shrinkage than the sample with no metal-organic additives in the temperature range up to 800°C. A larger final total shrinkage was produced (29%) as compared to that of pure silver film.

For silver film with MO-Zn added, it was observed that little shrinkage occurs before 600°C. However, as the sintering temperature increases over 600°C, the silver-based film shrinks rapidly with temperature. The final total shrinkage was about 23%. In the case of

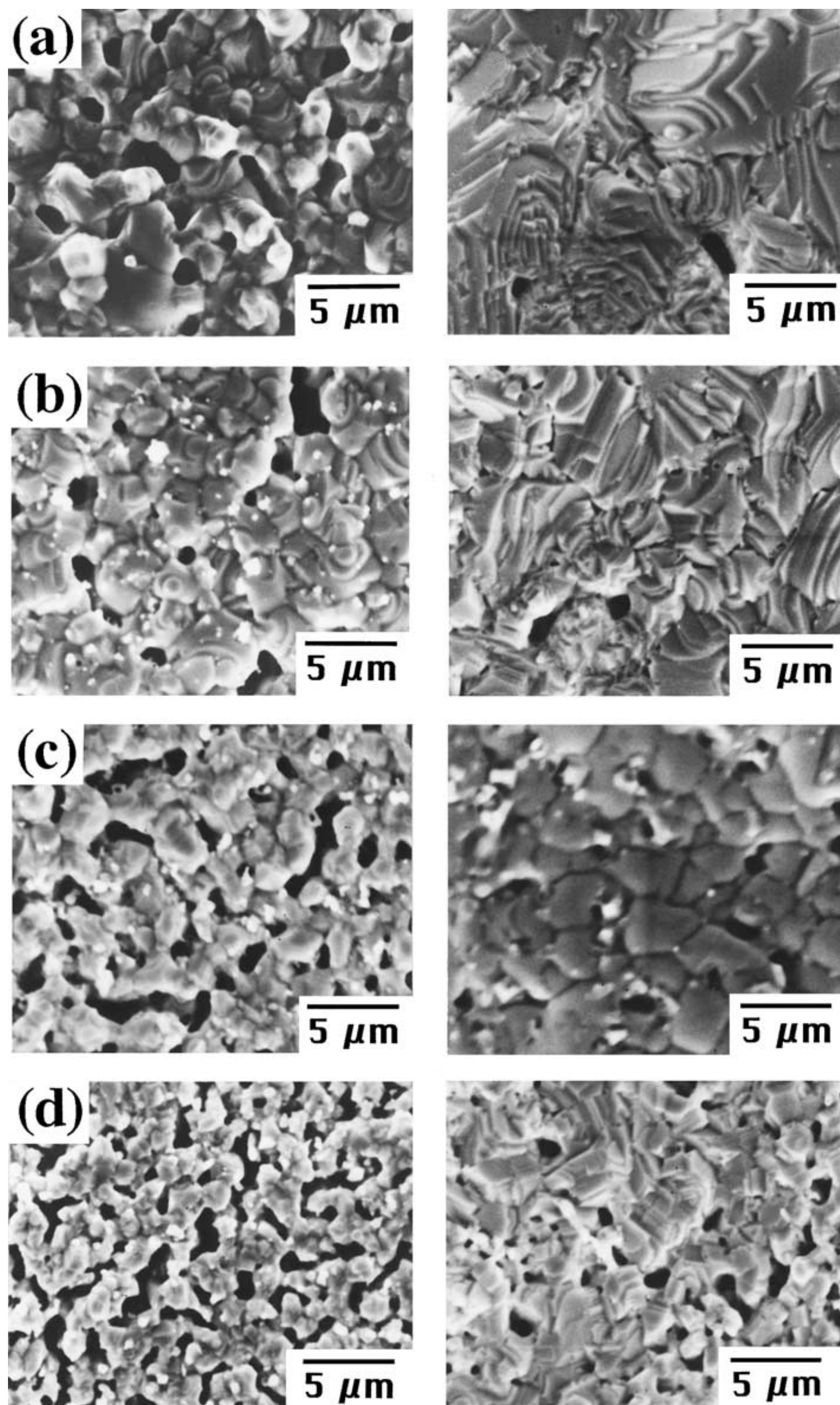

Figure 4 Microstructure changes in silver films added with 1 wt% (a) WO_3, (b) Fe_2O_3, (c) ZnO and (d) ZrO_2 by sintering at 600°C (left) and 800°C (right) for 0.5 h.

MO-Zr, although the sintering shrinkage of the silver film increases with increasing temperature, no apparent shrinkage was observed before 600°C. Furthermore, less total shrinkage occurs in the temperature range up to 800°C, resulting in less sintering shrinkage mismatch with the dielectric. In addition, the shrinkage amount of the silver-based films was also dependent on the added amount of MO-Zr. As shown in Fig. 6, the thermal shrinkage was performed for both dielectric tape and 1.5 wt% MO-Zr-added silver film from room temperature heated to 950°C with a ramp rate of 5°C/min and then held for 2 hrs. The sintering mismatch was much reduced between the dielectric and MO-Zr added-silver film.

Fig. 7 shows the surface micrographs for both silver films with 1wt% MO-W and MO-Zr added,

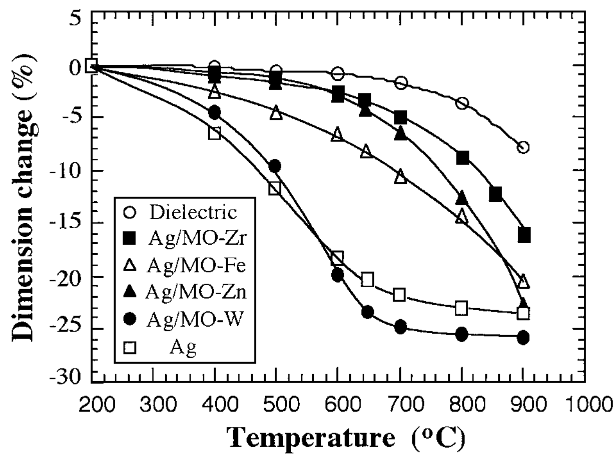

Figure 5 Thermal shrinkage characteristics of silver films with metal-organic precursors added at a heating rate of 5°C/min.

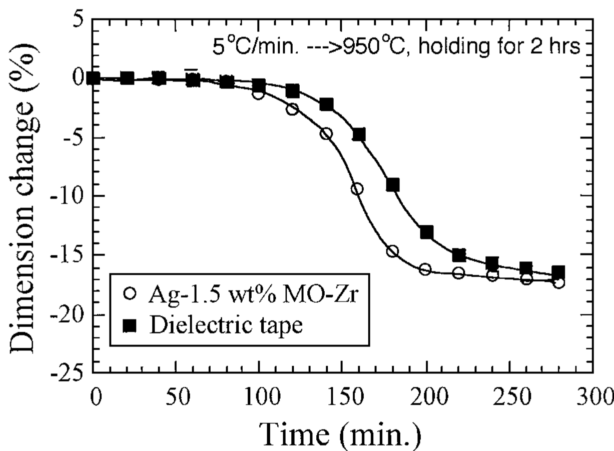

Figure 6 Compatible thermal shrinkage of 1.5 wt% MO-Zr-added silver film and dielectric tape.

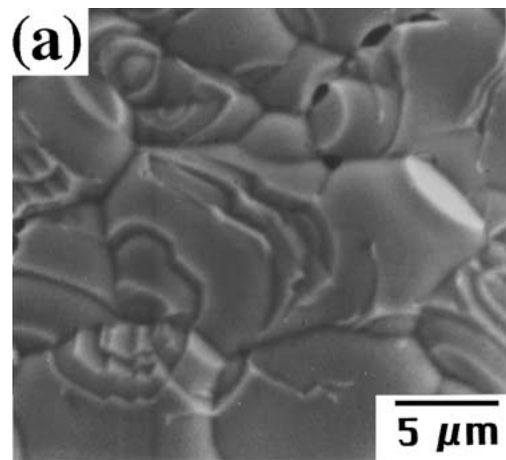

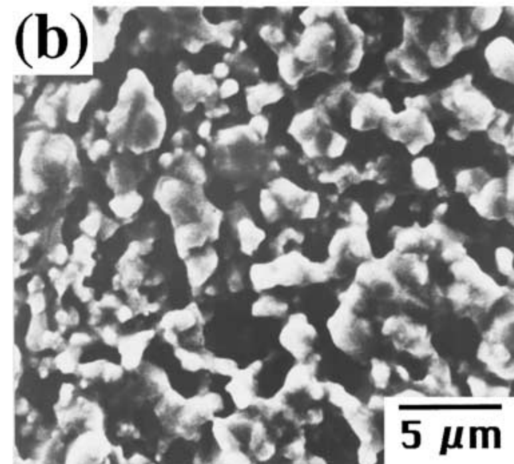

Figure 7 Surface microstructure of silver films added with 1 wt% (a) MO-W and (b) MO-Zr sintered at 600°C for 0.5 h.

respectively. The microstructure for the former silver-based film not only exhibits flat with array of parallel steps but also shows larger grain size (Fig. 7a). The grain size in MO-W-added silver film fired at 600°C was about 12 μm, larger than that in pure silver film (~7 μm). On the other hand, for the MO-Zr added silver film, a porous microstructure consisting of small grains with little sintering densification was observed in Fig. 7b.

3.4. Conductivity of silver-based films

The conductivity of internal electrode on the microwave properties of dielectric ceramics at high frequencies plays an important role. In order to evaluate the effect of metal oxides or metal-organic precursors on the conductivity of silver-based films, a "T-pattern" microstrip resonator was used. As observed in Fig. 8 for the silver films added with 1 wt% metal oxides or metal-organic precursors (MO), the conductivity of most silver-based films except MO-W added was apparently reduced.

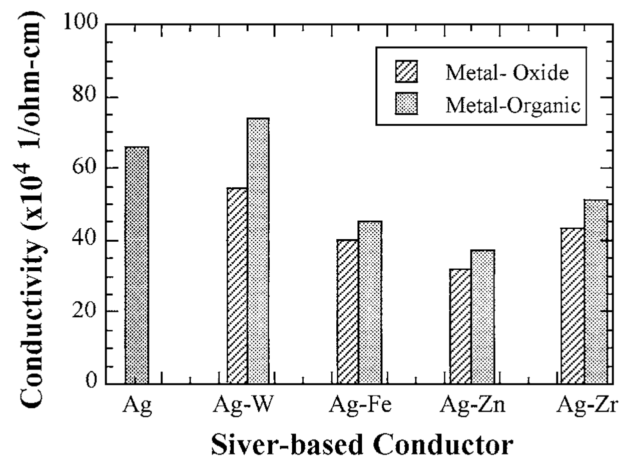

Figure 8 Conductivity comparison of silver films with a variety of metal oxides and metal-organic precursors added.

4. Discussion

4.1. Retardation of sintering shrinkage

The amount of shrinkage in the temperature range from room temperature to 800°C is the critical factor in forming delaminations in multilayer ceramic capacitors since the silver film begins to density, yet the dielectric has not begun to sinter and shrink. So, any remaining shrinkage in the silver film occurring above 800°C is of less consequence since this is the range in which the dielectric also shrinks. As the silver films were added with a variety of metal oxides, different sintering shrinkage was obtained (Fig. 3). It was believed that the sintering behavior was dependent on the characteristics of metal oxide, i.e., melting point of metal oxide. For example,

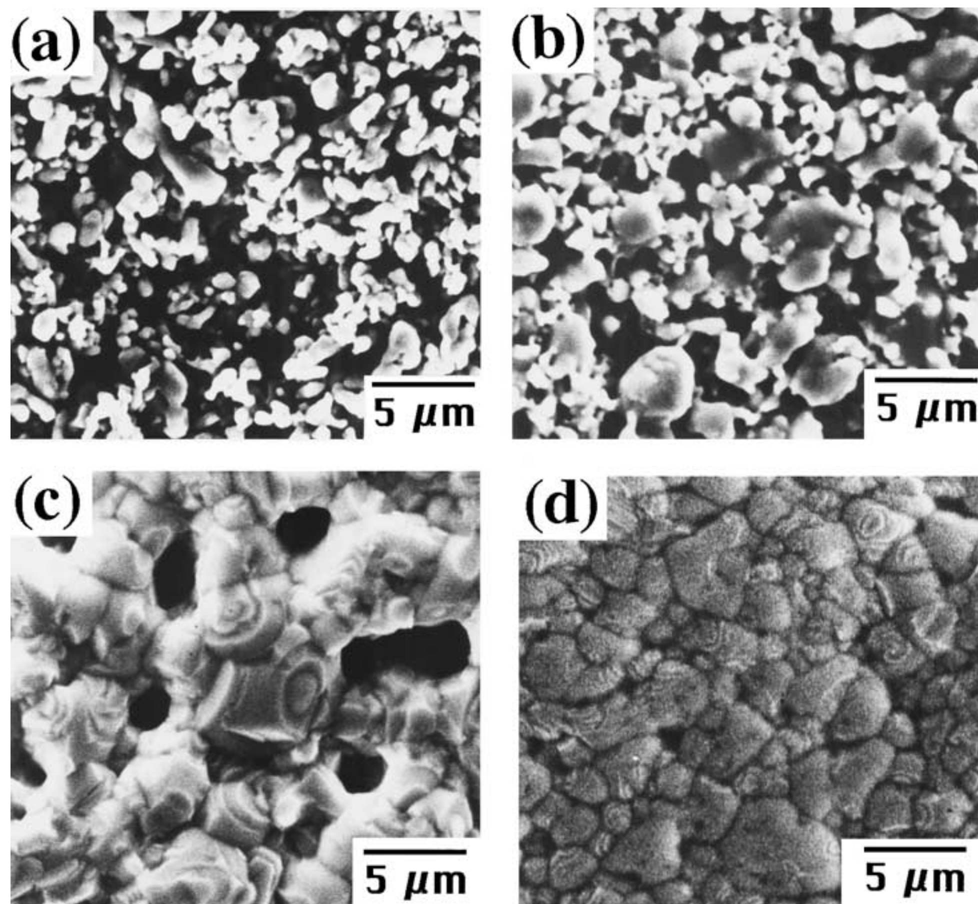

Figure 9 Surface microstructure of silver films with 1.5 wt% MO-Zr additive changes with sintering temperatures at (a) 400°C, (b) 600°C, (c) 800°C, and (d) 950°C for 0.5 h.

ZrO_2 additive exhibits a remarkable inhibition on sintering shrinkage of silver films in comparison to other metal oxides investigated in this work. It was strongly believed that the observed behavior in ZrO_2-added silver film was correlated with its higher refractory character.

Further comparison of the sintering shrinkage between Figs 3 and 5 revealed that metal oxide-added silver films exhibit a two-stage sintering shrinkage, which is completely different from the one-stage continuous shrinkage in the silver films added with metal-organic precursors. For the silver films with metal oxide added, the first-stage shrinkage can be thought due to the sintering densification of aggregate silver powders because the metal oxide powder can not be uniformly distributed over all the silver particles, as observed in Fig. 4c. Therefore, some local inhomogeneous densification and necking between silver powder takes place at the lower temperatures, i.e., 400–600°C. As increasing temperature, the aggregate silver particles coalesce and grow together in this second-stage at 600–800°C.

On the other hand, for the silver films added with metal-organic precursors, the shrinkage behavior can be elucidated from the microstructure evolution with 1.5 wt% MO-Zr-added silver films (Fig. 9). A possible mechanism for one-stage sintering shrinkage could be explained as follows. As the silver powder was mixed with MO-Zr precursor, the silver powder could be coated with a uniform layer of Zr-precursor. According to the report of Chu *et al.* [20], the MO-Zr film will be decomposed into an armophous structure at 400–450°C and crystallization occurs at ∼500°C with nano-sized ZrO_2 powder being formed. It stands to reason that as fired at 400°C, the metal-organic-doped silver films were more porous (Fig. 9a) prior to appreciable sintering (as expected, given the relatively high amount of organic to be removed) than the metal-oxide-doped films. Indeed, the convex shape of the MO-Zr (or MO-Fe, MO-Zn) doped specimens in Fig. 5 is similar to the initial convex shape seen (e.g., at <600°C) in the shrinkage curves of the ZrO_2, Fe_2O_3, and ZnO doped films in Fig. 3. At 600°C, Fig. 9b shows some of silver particles aggregate along with nano-sized ZrO_2 particles (marked with the arrows) distributed around or interleaved between silver powders. With increasing the sintering temperature to 800°C, although the grain coalescence of silver particles constantly takes place, a porous structure resulted as one can see in Fig. 9c, which indicates that the sintering densification of silver powder was apparently inhibited. At 950°C, a dense microstructure with smaller grain size (∼3 μm) was obtained (Fig. 9d) because the grain growth was obviously hampered as compared with that of silver powder with no MO-Zr. Consequently, the shrinkage mismatch can be apparently reduced.

4.2. Role of additives in conductivity

Generally, it was believed that as additives were added to silver, irrespective of whether these additives are

metals, glass or other metal oxides, the conductivity would be diminished. However, our results show that it was reverse for silver film with MO-W added. The conductivity measured for MO-W-added silver film exhibits slightly higher than pure silver film. The unique phenomenon observable can be reasonably explained as follows. As well known, W has the characteristics of variable valences. As the MO-W added silver film was sintered at 600°C. A dense microstructure with larger grain size can be obtained (Fig. 7a) in comparison with silver films with no additive and WO_3-added. Also there exists an obvious contrast across the grain boundaries, which further indicates a possibly partial dissolution of W into Ag. Leung *et al*. reported that the addition of 35–62 vol% of tungsten could increase the welding tendency of silver-tungsten [21]. These might imply that silver-tungsten tends to form a solid solution. Therefore, a unique microstructure and conductivity behavior was detected in MO-W added silver film.

5. Conclusions

1. The addition of metal oxide powders shows inferior to metal-organic precursors in reducing shrinkage of silver-based electrode.
2. The use of oxide powder additive shows two-stage shrinkage behavior in contrast to one-stage continuous shrinkage occurred in silver films with metal-organic precursors added.
3. The metal-organic precursors except for MO-W can be effectively decorated around silver powder and inhibits the sintering densification.
4. The shrinkage mismatch between silver-based films and dielectric ceramic can be much reduced with the addition of MO-Zr.
5. The unique conductivity and grain growth of silver film with 1 wt% MO-W added was possibly due to the partial dissolution of W into Ag.

Acknowledgment

The author would like to thank the financial support from the National Science Council of the Republic of China under Contract No. NSC88-2213-E-009-131.

References

1. K. WAKINO, in Proceedings of 6th IEEE International Symposium on Applications of Ferroelectrics (1986) p. 97.
2. H. OUCHI and S. KAWASHIMA, *Jpn. J. Appl. Phys.* **24** (Supplement 24-2) (1985) 60.
3. K. MATSUMOTO, T. HIUGA, K. TAKADA and H. ICHIMURA, in Proceedings of 6th IEEE International Symposium on Applications of Ferroelectrics (1986) p. 118.
4. I. BURN and W. C. PORTER, in “Ceramic Transactions, Vol. 15—Materials Processes for Microelectronic Systems,” edited by K. M. NAIR, R. POHANKA and R. C. BUCHANAN (American Ceramic Society, Westerville, OH, 1990) p. 385.
5. R. L. KEUSSEYAN, M. H. LABRANCHE and K. W. HANG, in ISHM Proceedings (1994) p. 185.
6. Z. WANG and S. ZHANG, in Proceedings of the 37th Electronic Components Conference, Catalog No. 87CH2448-9 (1987) p. 413.
7. S. F. WANG, J. P. DOUGHERTY, W. HUEBNER and J. G. PEPIN, *J. Amer. Ceram. Soc.* **77** (1993) 3051.
8. C. Q. LU, R. C. SUTTWELIN and T. K. GUPTA, *ibid.* **76** (1993) 1907.
9. J. G. PEPIN, W. BORLAND, P. O’CALLAGHAN and R. J. S. YOUNG, *ibid.* **72** (1989) 2287.
10. G. TMANDL and A. STIEGELSCHMIT, *Ber. Dtsch. Keram. Ges.* **56** (1976) 337.
11. K. I. YAJIMA and T. TAMAGUCHI, *J. Mater. Sci.* **19** (1984) 777.
12. H. T. SAWHILL, in “Advanced in Ceramics, Vol. 26—Ceramic Substrates and Packages for Electronic Applications,” edited by M. F. Yan, H. M. O’Bryan, Jr. K. Niwa and W. S. Young (American Ceramic Society, Westerville, OH, 1990) p. 307.
13. C. Y. KUO, *Solid State Tech.* Feb. (1974) 49.
14. J. P. PEPIN, US Patent no 4954926 (1990).
15. M. J. POPOWWICH, US Patent no. 4075681 (1978).
16. J. C. CONSTANTINE, European Patent no. 0394037 (1990).
17. D. I. AMEY and J. CURILLA, in Proceedings of the 41st Electronics Component Conference (1991) p. 267.
18. K. YATA and T. YAMAGUCHI, *J. Amer. Ceram. Soc.* **75** (1992) 2910.
19. A. O. ALI, R. B. KSHIRAGAR and C. V. DHARMADHIKARI, *Thin Solid Films* **323** (1998) 105.
20. P.-Y. CHU and R. C. BUCHANAN, *J. Mater. Res.* **6** (1991) 1736.
21. C. H. LEUNG and P. C. WINGERT, in Proceedings of the 33rd Meeting of the IEEE Holm Conference on Electrical Contacts (1987) p. 133.

Received 24 July 2000
and accepted 8 August 2001